Modulation of the Binding Affinity of Myelopoietins for the Interleukin-3 Receptor by the Granulocyte Colony-Stimulating Factor Receptor Agonist

William F. Hood,* Yiqing G. Feng, Roger J. Schilling, Yatin Gokarn, Cindy Jarvis, Edward E. Remsen, Jeng-Jong J. Shieh, William Joy, Barbara K. Klein, Joseph O. Polazzi, Joseph K. Welply, John P. McKearn, and Joseph B. Monahan

Searle Research and Development, Pharmacia Corporation, 700 Chesterfield Parkway North, St. Louis, Missouri 63198

Received March 23, 2001; Revised Manuscript Received July 23, 2001

ABSTRACT: Myelopoietins (MPOs) are a family of recombinant chimeric proteins that are both interleukin-3 (IL-3) receptor and granulocyte colony-stimulating factor (G-CSF) receptor agonists. In this study, MPO molecules containing one of three different IL-3 receptor agonists linked with a common G-CSF receptor agonist have been examined for their IL-3 receptor binding characteristics. Binding to the α-subunit of the IL-3 receptor revealed that the affinity of the MPO molecules was 1.7−3.4-fold less potent than those of their individual cognate IL-3 receptor agonists. The affinity decrease was reflected in the MPO chimeras having approximately 2-fold slower dissociation rates and 2.7−5.5-fold slower association rates than the corresponding specific IL-3 receptor agonists alone. The affinity of binding of the MPO molecules to the heteromultimeric $\alpha\beta$ IL-3 receptor expressed on TF-1 cells was either 3-, 10-, or 42-fold less potent than that of the individual cognate IL-3 receptor agonist. Biophysical data from nuclear magnetic resonance, near-UV circular dichroism, dynamic light scattering, analytical ultracentrifugation, and size exclusion chromatography experiments determined that there were significant tertiary structural differences between the MPO molecules. These structural differences suggested that the IL-3 and G-CSF receptor agonist domains within the MPO chimera may perturb one another to varying degrees. Thus, the differential modulation of affinity observed in IL-3 receptor binding may be a direct result of the magnitude of these interdomain interactions.

Interleukin-3 (IL-3)[1] and granulocyte colony-stimulating factor (G-CSF) are cytokines which stimulate the proliferation and differentiation of hematopoietic cells. IL-3, or multicolony stimulating factor, promotes the differentiation of multipotent progenitor cells into the granulocyte, monocyte, erythroid, and megakaryocyte lineages (*1*, *2*). G-CSF, on the other hand, specifically stimulates the proliferation, differentiation, and maturation of myeloid progenitor cells of the neutrophil lineage (*3*). When used in combination, IL-3 and G-CSF have been shown to have an advantage over using either of them alone in the treatment of neutropenia and thrombocytopenia as a result of cancer chemotherapy, bone marrow transplant, or congenital defects (*4*−*7*). Myelopoietin (MPO) proteins, which have been engineered to contain both IL-3 and G-CSF receptor agonist activities, demonstrate synergistic hematopoietic activities that exceed those observed by a combination of G-CSF and IL-3 (*8*). MPO proteins were shown to be superior to the two single molecules in both cellular (colony-forming unit activity in $CD34^+$ cells derived from human bone marrow) and in vivo (mobilization of peripheral blood progenitor cells in nonhuman primates) assays (*9*, *10*). Furthermore, clinical trials have indicated that the MPO molecules are well-tolerated in humans and are effective in mobilizing neutrophil and multilineage precursors in patients undergoing chemotherapy (*11*−*13*).

Single molecules possessing dual agonist activity have been described previously. Those molecules have variable activity compared with the individual agonists (*14*−*19*). For example, a chimera of IL-3, bombyxin, and human insulin-like growth factor II was reported to be 25−30 times more active than IL-3 in a proliferation assay of the human proerythroleukemic cell line TF-1 (*14*). PIXY321, in which IL-3 and GM-CSF were combined (*15*), exhibited enhanced receptor affinity and in vitro proliferative activity compared to either cytokines alone or in combination. In contrast, when IL-3 and erythropoietin were fused (*16*), no enhancement of erythropoiesis over that observed with the combination of the individual cytokines could be shown. These prior studies demonstrate that the biological activity and receptor binding activity of the dual receptor agonist proteins depend on the complementarity of the biological profiles of the cytokines, as well as the linker and the orientation, i.e., the sequential order, of the cytokines that are engineered into the chimeras.

* To whom correspondence should be addressed. Phone: (636) 737-6564. Fax: (636) 737-6599. E-mail: william.f.hood@pharmacia.com.

[1] Abbreviations: MPO, myelopoietin; IL-3, interleukin-3; G-CSF, granulocyte colony-stimulating factor; GM-CSF, granulocyte/macrophage colony-stimulating factor; IL-5, interleukin-5; CD, circular dichroism; EDTA, ethylenediaminetetraacetic acid; FBS, fetal bovine serum; RAMFc, rabbit anti-mouse Fc; HEPES, *N*-(2-hydroxyethyl)-piperazine-*N*′-2-ethanesulfonic acid; HBS, HEPES-buffered saline; PBS, phosphate-buffered saline; NMR, nuclear magnetic resonance; HSQC, heteronuclear single-quantum coherence; SEC, size exclusion chromatography; DLS, dynamic light scattering; SE, sedimentation equilibrium; SV, sedimentation velocity.

10.1021/bi010590t CCC: $20.00
Published on Web 10/17/2001

Table 1: Myelopoietins Examined for IL-3 Receptor Binding Affinity

compound	N-terminal agonist	linker[a]	C-terminal agonist
MPO A	SynIL-3 A[b]	L1	G-CSF (S17)
MPO B	SynIL-3 B[c]	L2	G-CSF (S17)
MPO C1	SynIL-3 C[d]	L1	G-CSF (S17)
MPO C2	SynIL-3 C[d]	L2	G-CSF (S17)
MPO C1R	G-CSF (S17)	L1	SynIL-3 C[d]
MPO C2R	G-CSF (S17)	L2	SynIL-3 C[d]

[a] The sequence of L1 is YVEGGGGSPGEPSGPISTINPSPPSKESHKSPNMA, and that of L2 is YVEGGGGSPGGGSGGGSNMA. [b] SynIL-3 A is comprised of residues 14−125 of hIL-3 with V14A and E50D mutations. [c] SynIL-3 B has residues 14−125 of hIL-3 with multiple mutations (sequence reported in ref *21*). [d] SynIL-3 C has residues 14−125 of hIL-3 with the following mutations: V14A, N18I, T25H, Q29R, L32A, F37P, G42D, Q45V, D46S, N51R, R55L, A60S, N62V, S67N, Q69E, A73G, S76A, K79R, L82Q, L87S, T93S, H98I, D101A, N105Q, R109E, K116V, N120Q, and A123E.

Through a systematic mutagenesis effort (*20*), we have engineered a series of hIL-3 receptor agonists, including SC-55494 (daniplestim) (*21*), exhibiting differentially enhanced hematopoietic activity relative to inflammatory activity, compared with native hIL-3. We have recently engineered a series of recombinant MPO molecules that are composed of either different IL-3 receptor agonists paired with the same G-CSF receptor agonist, or different G-CSF receptor agonists paired with the same IL-3 receptor agonist. A study examining MPO molecules containing various G-CSF receptor agonists coupled to a single IL-3 receptor agonist has been reported elsewhere (*22*). In the study presented here, we examined the effect of the G-CSF receptor agonist motif, the protein linker, and the agonist orientation on the IL-3 receptor binding properties of the MPO proteins (Table 1). To correlate structure with function, biophysical characteristics of the MPO proteins were examined using circular dichroism spectroscopy, NMR spectroscopy, dynamic light scattering, analytical ultracentrifugation, and size exclusion chromatography. The results presented in this study establish that the potency of an IL-3 receptor agonist is modulated, independent of linker and orientation, in an MPO chimera. These results further suggest that within a particular MPO chimera, the intramolecular interaction between the two agonist domains may be responsible for the modulation of the IL-3 receptor binding affinity. The degree of interaction between the domains appears to be related to the sequence of the IL-3 receptor agonist.

EXPERIMENTAL PROCEDURES

Construction, Expression, and Purification of Myelopoietins. The general DNA manipulation, construction, expression, and purification of the recombinant proteins (including ^{15}N-labeled proteins) from *Escherichia coli* have been previously described (*20*, *23*). Briefly, inclusion bodies were isolated by sonication of the *E. coli* cell pellets in 10 mM Tris (pH 8.0), 1 mM EDTA buffer, followed by centrifugation. The inclusion bodies from a 1 L fermentation were solubilized in 30 mL of 8 M urea, 50 mM Tris, and 5 mM dithiothreitol (pH 9.5) and stirred at room temperature for 30 min. To initiate and complete the refolding, 210 mL of another buffer containing 2.3 M urea and 50 mM Tris (pH 9.5) was added and the mixture allowed to stir for 24 h at 4 °C. Refolding was terminated by adjusting the pH to 5.0 with 15% acetic acid. The refolded proteins were further purified via either reverse-phase HPLC (Vydac C_{18}) or ion exchange chromatography to greater than >98%, as determined by sodium dodecyl sulfate−polyacrylamide gel electrophoresis (*24*). The protein concentrations were determined by reverse-phase HPLC, amino acid composition, and UV absorption.

Cell Line and Reagents. The human proerythroleukemic cell line, TF-1 (American Tissue Culture Collection, Rockville, MD), expressing the IL-3 receptor was maintained in RPMI 1640 medium with 10% heat-inactivated FBS and IL-3 (2 ng/mL). FBS was purchased from Harlan (Indianapolis, IN) and cell culture medium from Gibco BRL (Grand Island, NY).

For IL-3 receptor α-subunit binding, a soluble fusion protein was generated containing the extracellular portion (amino acids 20−305) of the human IL-3 (hIL-3) receptor α-subunit linked to the Fc portion of murine IgG_{2a} (α-Fc). This protein was produced in a 10 L bioreactor seeded with Sf9w cells (a clonal isolate of the IPLB-SF21-AE cell line derived from the pupal ovarian tissue of the fall army worm, *Spodoptera frugiperda*) at an initial cell density of 2.5×10^5 cells/mL. The bioreactor was maintained at 27 °C; its contents were stirred at 60 rpm, and the level of dissolved oxygen was controlled at 50% of the atmospheric air saturation. The Sf9w insect cell culture was infected with recombinant baculovirus encoding hIL-3 receptor α-Fc at 0.1 pfu/cell at a cell density of $0.5-1.0 \times 10^6$ cells/mL. The contents of the bioreactor were harvested approximately 72−96 h postinfection by centrifugation.

IL-3 Receptor Binding. Prior to the receptor binding experiments, the TF-1 cells containing the IL-3 receptor α- and β-subunits ($IL\text{-}3R_{\alpha/\beta}$) were starved of IL-3 overnight by exchanging their IL-3-containing growth medium with medium devoid of the cytokine. On the day of the assay, cells were washed at 0−4 °C by centrifugation (600*g* for 12 min) and the resulting cell pellet was resuspended in fresh RPMI 1640 medium. The washing procedure was repeated three times, with the final cell pellet being resuspended in ice-cold assay medium (Iscove's Modified Dulbecco's Medium with 5% FBS and 0.2% sodium azide) to yield approximately $2-4 \times 10^6$ cells per sample incubation. All binding experiments were performed at 0−4 °C. Assay incubations (0.1 mL) containing the radiolabeled IL-3 receptor agonist [^{125}I]SC-65461 (*21*) and a competing compound were initiated by the addition of cells which had been kept at 0−4 °C for at least 20 min to minimize any internalization. Incubations were halted by separation of the bound and free radiolabeled ligand by rapid centrifugation (12000*g* for 1 min) in an Eppendorf 5415C centrifuge. The supernatant was aspirated and the tube tip containing the cell pellet with the associated radioactivity cut off and counted in an ICN Micromedics System automatic gamma counter. Nonspecific binding was defined as the residual binding occurring in the presence of excess SynIL-3 B (1000 nM). [^{125}I]SC-65461 competition binding experiments using 50−100 pM radiolabeled ligand were analyzed using Scatchard and Hill transformations and the IC_{50} values for compounds determined using logit-log analysis.

Surface Plasmon Resonance. Samples were analyzed on a BIACORE 2000 surface plasmon resonance instrument

from Pharmacia Biosensor AB (Uppsala, Sweden). The sensor chip CM5, amine coupling kit, rabbit anti-mouse Fc antibody (RAMFc), and *N*-(2-hydroxyethyl)piperazine-*N*′-2-ethanesulfonic acid (HEPES)-buffered saline (HBS) were purchased from Pharmacia (Piscataway, NJ). All samples were centrifuged at 5560*g* for 15 s to eliminate any air trapped in the solution before analysis. The running buffer consisted of 10 mM HEPES (pH 7.4), 150 mM NaCl, 3.4 mM EDTA, and 0.005% (v/v) surfactant P20.

For sample analysis at 25 °C, two flow cells were monitored simultaneously: a blank, containing no RAMFc agent, and an active cell which had RAMFc immobilized on the sensor chip surface via amine coupling chemistry. During each run, an active or regenerated RAMFc surface was exposed to a 6 min injection of the IL-3 receptor α-Fc solution at a flow rate of 10 μL/min. The surface was then washed for 25 min with running buffer, after which the flow rate was changed to 20 μL/min and the sample (25−1000 nM) injected for 3 min. The chip surface was regenerated with a 3 min injection of 1.0 N formic acid. The association and dissociation regions of the receptor−ligand interaction were fit with a kinetics global analysis evaluation program supplied with the BIACORE system.

Circular Dichroism. Circular dichroic measurements were taken using a JASCO 500C spectropolarimeter. The near-UV (250−340 nm) spectra were obtained in a 1 cm path, thermojacketed, quartz cell. All data are calculated as the mean residue ellipticity and expressed as molar ellipticity. All spectra were obtained at 20 °C. The instrument was calibrated using *d*-(+)-10-camphorsulfonic acid. The spectral additivities of the IL-3 and G-CSF receptor agonists were determined using a dual-chamber thermojacketed, optical cell. This allowed the individual protein solutions to be separately measured and then mixed. The mixed solution was measured a second time to investigate subtle spectral changes induced by mixing. The data plotted as the spectral sum include the CD spectra of the linker, L1 or L2 (see Table 1) at pH 7.5. Protein concentrations were determined by using light scattering-corrected absorbance at 280 nm. The molar extinction coefficients were determined using literature values for the ultraviolet absorbances of tryptophan, tyrosine, and a disulfide bond in neutral aqueous solution (*25*). These measurements were taken using a Hewlett-Packard 88451A diode array spectrophotometer at ambient temperature. All spectral measurements of protein solutions were taken in 10 mM Tris (pH 7.5) or, when noted, in 10 mM sodium acetate (pH 4.0).

Size Exclusion Chromatography. High-performance size exclusion chromatography (SEC) was carried out using a Superose 12 column (1.2 cm × 30 cm; Pharmacia) equilibrated in phosphate-buffered saline (PBS). The column was developed at a flow rate of 0.5 mL/min with the elute monitored at 214 nm. Samples were diluted to 0.5 mg/mL in PBS, and the injection volume was 100 μL. The column was calibrated daily with molecular mass standards (Bio-Rad, Richmond, CA) ranging from 1350 to 670 000 Da. The apparent molecular masses of the MPO molecules were determined by comparing elution times to those of molecular mass standards.

Dynamic Light Scattering. The hydrodynamic diameter distribution was determined at 21 °C using dynamic light scattering (DLS) experiments on a Brookhaven (Holtsville, NY) system which consists of a model BI-200SM goniometer, a model EMI-9865 photomultiplier, and a model BI-9000AT digital correlator. Incident light was provided by a model 95-2 Ar ion laser (Lexel Corp., Palo Alto, CA) operating at 514.5 nm. Protein solutions prepared in PBS and Tris buffers were centrifuged to remove dust particles prior to the measurements.

Scattered light was collected at a fixed angle of 90°. The digital correlator was operated with 522 channels, a ratio channel spacing with an initial delay time of 1 μs, a final delay time of 10 ms, and a duration time of 2 min. A photomultiplier aperture of 400 μm was used, and the incident laser intensity was adjusted to obtain a photon counting rate of at least 200 kcps. Only measurements in which measured and calculated baselines of the intensity autocorrelation function agreed to within 0.1% were used to calculate particle sizes. The particle size distribution and distribution average were calculated with the ISDA software package provided by the vendor, which employed single-exponential fitting, cumulants analysis, and non-negatively constrained least-squares particle size distribution analysis routines. Reported particle size distribution averages are mean values of five independent determinations.

Analytical Ultracentrifugation. Sedimentation equilibrium (SE) and sedimentation velocity (SV) experiments were conducted at 20 °C in a Beckman model XL-I analytical ultracentrifuge equipped with a Ti-55 eight-hole rotor on samples in Tris and PBS buffers. Sedimentation velocity experiments were performed on samples containing 1 mg/mL protein in Tris and 0.66 mg/mL protein in PBS using a cell assembled with an Epon charcoal-filled, double-sector centerpiece and sapphire windows. The sedimentation patterns were monitored using the on-line absorbance optical system at 280 nm, and the data were analyzed using SVEDBERG (*26*, *27*).

For the sedimentation equilibrium experiments, a six-channel, Epon charcoal-filled centerpiece was used. The equilibrium concentration profile was obtained using the interference optical system. Experiments were performed with three concentrations (0.66, 0.33, and 0.165 mg/mL) at four rotor speeds (10 000, 15 000, 20 000, and 25 000 rpm). The data were analyzed using NONLIN (*28*). Partial specific volumes for the proteins were calculated on the basis of amino acid composition (*29*).

Nuclear Magnetic Resonance. All nuclear magnetic resonance (NMR) spectra were recorded at 25 °C on a Varian UNITY-500 spectrometer equipped with a pulsed field gradient unit. Samples were either dissolved directly or exchanged into a buffer containing 10 mM potassium phosphate at pH 7 or a buffer containing 50 mM acetate-d_4 at pH 4 by using PD-10 Sephadex G25M prepacked columns (Pharmacia) or Centricon 10 (Amicon). The final concentrations used to record the one-dimensional proton spectra were 0.07−0.5 mM, and the final pHs were 7.0−7.2 and 3.9−4.1. Solvent suppression was achieved by low-power preirradiation at the solvent frequency, or WATERGATE (*30*). $^{15}N-^{1}H$ heteronuclear quantum coherence (HSQC) spectra (*31*) were collected on samples containing 0.3−0.5 mM ^{15}N-labeled MPO A, MPO B, SynIL-3 A, SynIL-3 B, and the G-CSF receptor agonist using acquisition times of 137 (F_2) and 240 ms (F_1, ^{15}N). The two-dimensional spectra were processed using VNMR (Varian, Palo Alto, CA).

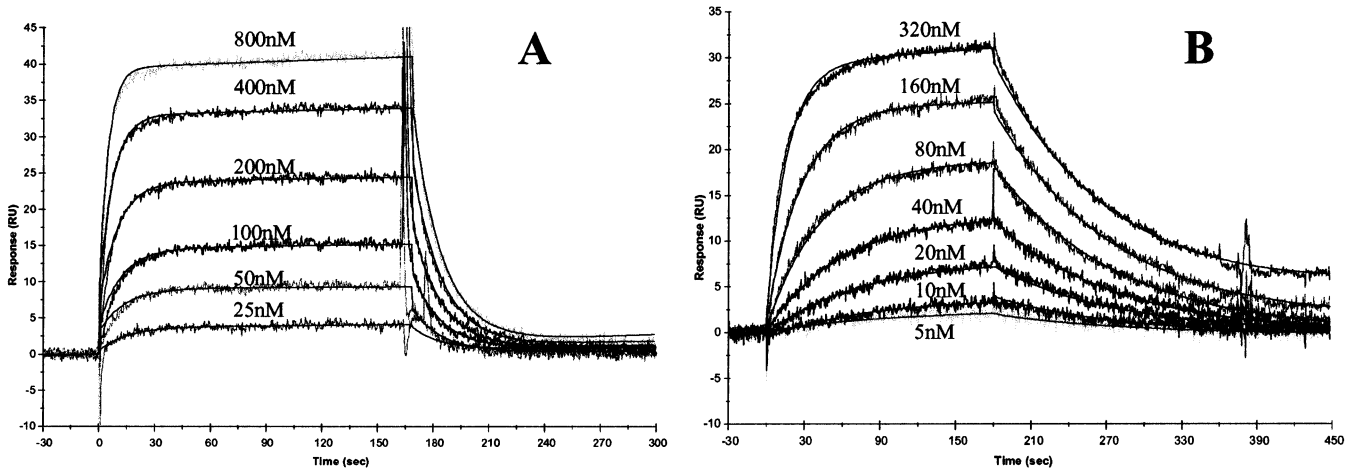

FIGURE 1: Biacore sensorgram of the binding of MPO A (A) and MPO B (B) to immobilized IL-3 receptor α-Fc.

RESULTS

Three classes of MPO proteins employing IL-3 receptor agonists containing various amino acid mutations were constructed and tested in this study (Table 1). The first class, MPO A (Leridistim) (*32*), contains a truncated hIL-3 (amino acids 14−125) with two amino acid substitutions, V14A and E50D (SynIL-3 A). The second class, MPO B, contains a truncated hIL-3 variant with multiple amino acid substitutions (SynIL-3 B). Both of these IL-3 receptor agonists have been previously reported to have increased IL-3 receptor binding activity and proliferative activity relative to the native IL-3 molecule (*21*, *33*). The third MPO class has a different, highly potent, multiply substituted IL-3 receptor agonist, SynIL-3 C (see the Table 1 footnote) (*34*). The MPO C class of proteins consists of molecules with reverse agonist orientation and linker length variations.

IL-3 Receptor Competitive Binding Studies. IL-3 exerts its effect on multilineage hematopoietic cell growth by binding to a cell surface receptor which consists of an α-subunit and a β-subunit (*35*, *36*). IL-3 binds to the α-subunit with low affinity, while it has no measurable affinity for the isolated β-subunit. A high-affinity complex, capable of signal transduction, is formed only in the presence of both α- and β-subunits. The characteristics of myelopoietin binding to both the high-affinity IL-3 receptor of TF-1 cells and the IL-3 receptor α-subunit were determined.

The binding of a radiolabeled, high-affinity IL-3 derivative, [^{125}I]SC-65461, to TF-1 cells containing the IL-3R$_{\alpha/\beta}$ was inhibited with low nanomolar affinity by native human IL-3, SynIL-3 A, B, and C, and the myelopoietins (Table 2). While all the MPO molecules inhibited the binding of [^{125}I]-SC-65461 to the IL-3 receptor with high potency, a decrease in the MPO affinity relative to that of their cognate IL-3 receptor agonist was observed. The extent of this decrease was dependent upon the specific IL-3 receptor agonist component of the MPO molecule. More specifically, the potency of MPO A for inhibiting binding to the IL-3 receptor was 3-fold lower than that of SynIL-3 A; MPO B was 42-fold less potent than SynIL-3 B, and MPO C1, C2, C1R, and C2R were 8−12-fold less potent than SynIL-3 C. While MPO A and B bind with lower affinity than hIL-3 to cells expressing the IL-3 receptor alone, MPO C is nearly equipotent.

Table 2: Inhibition of [^{125}I]SC-65461 Binding to the IL-3 Receptor Expressed on TF-1 Cells ($\alpha\beta$ Complex)[a]

compound	IC_{50} (nM)	compound	IC_{50} (nM)
hIL-3	3.1 ± 0.7 (6)	SynIL-3 C	0.24 ± 0.03 (5)
SynIL-3 A	5.8 ± 1.3 (5)	MPO C1	2.4 ± 0.3 (3)
MPO A	18 ± 3 (4)	MPO C2	2.8 ± 0.3 (3)
SynIL-3 B	0.38 ± 0.04 (6)	MPO C1R	2.2 ± 0.1 (3)
MPO B	16 ± 3 (4)	MPO C2R	1.9 ± 0.2 (3)

[a] Inhibitory potency measured at 4 °C is expressed as the mean ± the standard error of the mean (nanomolar) of the specified compound as determined using logit-log analysis. The number in parentheses indicates the number of experiments.

Within the MPO C class, the effect of both linker length and orientation was examined. Both MPO C1 and MPO C2 have similar orientations, with the domain of SynIL-3 C located at the N-terminal region of the molecules, but employ linkers of 35 residues (L1) and 20 residues (L2), respectively (see Table 1). The lack of a significant difference in binding potency between MPO C1 and MPO C2 (Table 2) indicated that for these linkers neither the linker length nor the linker composition affected binding. The MPO C2R molecule which has the opposite orientation compared with MPO C2 (SynIL-3 C domain at the C-terminus) demonstrated a slight increase in binding affinity (1.9 ± 0.2 vs 2.8 ± 0.3 nM; $p < 0.05$) compared with MPO C2. A less pronounced trend between MPO C1 and MPO C1R was observed.

Kinetic Rate Constants for Binding to the α-Subunit of the IL-3 Receptor. The kinetics of the interaction of the MPO molecules with the IL-3 receptor α-subunit were examined using surface plasmon resonance (Table 3). Representative sensorgrams for MPO A and MPO B are shown in Figure 1, and the data indicate that the dissociation rates of the IL-3 receptor agonists vary by 30-fold. The kinetic dissociation rates for the MPO are approximately half those of their respective IL-3 receptor agonist counterparts. This trend exists irrespective of the IL-3 receptor agonist, orientation, or linker used in the MPO protein.

The association rates show more variation between MPO and their cognate IL-3 receptor agonist. All MPO molecules had slower association rates than their respective IL-3 receptor agonists. MPO A exhibited a nearly 3-fold slower association rate compared with that of SynIL-3 A; MPO B had a 5.5-fold decrease in rate relative to that of SynIL-3 B,

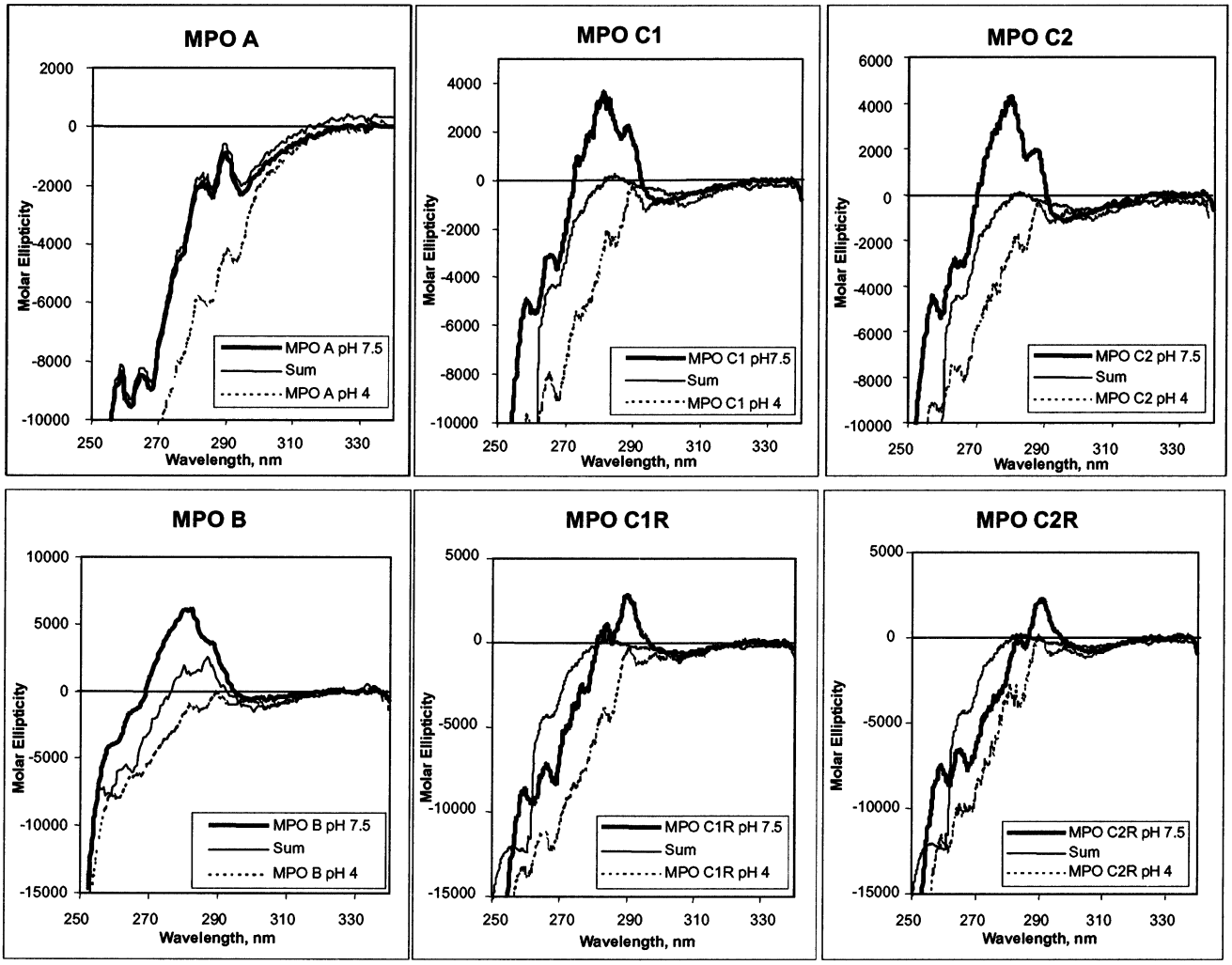

FIGURE 2: Near-UV CD spectra of MPO molecules at pH 7.5 (thick lines) and 4.0 (dashed lines). Also shown are the summed spectra of the corresponding components, including the linker (thin lines), recorded in 10 mM Tris (pH 7.5).

Table 3: Kinetic Rate Constants of Myelopoietins and SynIL-3 for Binding to the IL-3 Receptor α-Fc[a]

compound	k_a ($\times 10^6$ M^{-1} min^{-1})	k_d ($\times 10^{-3}$ min^{-1})	K_d (nM)
hIL-3	5.5 ± 1.7 (5)	6600 ± 700 (5)	1200
SynIL-3 A	27 ± 4 (6)	5460 ± 100 (6)	202
MPO A	10 ± 2 (5)	3420 ± 170 (6)	342
SynIL-3 B	60 ± 3 (18)	1500 ± 60 (18)	25
MPO B	11 ± 1 (4)	660 ± 40 (4)	60
SynIL-3 C	40 ± 0.4 (2)	350 ± 40 (2)	9
MPO C1	7.8 ± 0.2 (6)	240 ± 10 (6)	31
MPO C2	7.2 ± 0.2 (6)	220 ± 10 (6)	31
MPO C1R	10 ± 0.3 (3)	250 ± 10 (3)	25
MPO C2R	14 ± 0.3 (3)	220 ± 10 (3)	16

[a] k_a is the association constant, k_d the dissociation constant, and K_d the equilibrium dissociation constant at 25 °C determined from steady-state analysis of the data. Data are expressed as the means ± the standard error of the mean (where applicable) from the number of experiments indicated in parentheses.

and the MPO C series had 3−6-fold slower association rates than SynIL-3 C. A small orientation effect was again observed between MPO C2 and MPO C2R; the association rate was slightly faster (2-fold) when the IL-3 receptor agonist moiety was located at the C-terminal portion of the molecule rather than at the N-terminal portion. A similar but less pronounced trend was seen with MPO C1 and MPO C1R.

Circular Dichroism Measurement. A variety of biophysical measurements were performed to study the structure of MPO proteins. Included in these experiments is evaluation of near-UV circular dichroism (CD), which reflects tertiary structure. The near-UV CD spectra of the MPO molecules are compared in Figure 2. All the MPO spectra show negative troughs at 268 and 262 nm. These troughs are phenylalanyl fine structure which appear ∼6 nm apart and have similar intensities of the same sign. The spectra of MPO B, C1, and C2 exhibit maxima at 288 and 281 nm. The spectra of MPO A, C1R, and C2R demonstrate a clear band at 290 nm, a trough at 285 nm, and a peak at 282 nm. It is difficult to interpret these bands without the crystal structure; however, the 0−0 ^1L_b band of tryptophan lies between 288 and 292 nm. In addition, characteristic tyrosyl vibronic structure can occur at 281 and 287−288 nm (*37*). Two important factors that can influence the CD spectra include interactions of the aromatic ring with its surrounding environment and the number of aromatic residues. Since all of the tested myelopoietins contain the same number of tryptophans and tyrosines (eight total), these differences between the spectra of MPO B, C1, and C2 and the spectra of MPO A, C1R, and C2R probably represent variances in the environmental interactions of the aromatic residues in the respective myelopoietins. These effects most likely reflect a chro-

Table 4: Apparent Molecular Masses of Myelopoietins from Size Exclusion Chromatography

compound	apparent molecular mass[a] (Da)	actual molecular mass (Da)
MPO A	41 440 (4)	34 823
MPO B	29 445 (3)	33 030
MPO C1	37 178 (3)	34 757
MPO C2	33 192 (3)	32 961
MPO C1R	39 907 (2)	34 757
MPO C2R	32 950 (2)	32 961

[a] Apparent molecular masses of MPO molecules were determined by comparing elution times to those of molecular mass standards. The number in parentheses refers to the number of separate determinations.

mophoric modification rather than a major conformation difference. Changing the pH from 7.5 to 4.0 uniformly decreased the intensity of the MPO A and MPO B spectra with concomitant retention of all bands. The largest change is evident in the MPO B spectra where the tyrosine band at 281 nearly disappears and suggests the tyrosine environments in MPO B are structurally more rigid. These observed CD alterations could arise from specific interaction of the two agonist domains within a chimeric MPO molecule. One piece of evidence supporting the interpretation of a specific interaction within the chimera is the CD spectrum of an equimolar mixture of the SynIL-3 B and the G-CSF receptor agonist. This spectrum can be superimposed on the numerical sum of the two individual agonist spectra (data not shown), suggesting the nonadditivity could be due to distinct structural features of the chimera. In contrast to this discussion of tertiary structure changes, the secondary structure of all myelopoietins exhibits only small differences (~3% change in helicity) when compared to the weighted sum spectra of the two components (data not shown).

Size Exclusion Chromatography. Size exclusion chromatographic elution profiles of the MPO molecules revealed that MPO B migrated with the longest retention time of all the MPO molecules that were tested, indicating the lowest apparent molecular mass, while MPO A eluted with the shortest retention time corresponding to the highest apparent molecular mass (Table 4). Intermediate retention times were observed with the MPO C series of molecules. The much shorter than expected retention time of MPO A is indicative of a species with a higher than predicted molecular mass (+7940 Da). The fact that the actual molecular masses of these molecules are similar on the basis of amino acid composition suggests that the different elution pattern may be attributed to differences in molecular shape with MPO B having the most compact structure of the MPO molecules.

Dynamic Light Scattering, Sedimentation Velocity, and Sedimentation Equilibrium. To confirm the molecular shape and size difference inferred from size exclusion chromatography analysis, we performed dynamic light scattering (DLS) and sedimentation velocity (SV) experiments on MPO A and MPO B, the two MPOs that exhibited the largest and smallest apparent molecular masses. Unlike SEC retention time experiments which measures relative molecular size, DLS and SV experiments provide absolute size determinations. Uncertainties in the correlation between molecular mass and molecular size and/or shape due to nonideal SEC effects such as adsorption, ion exclusion, and ion exchange are eliminated through the use of DLS and SV methods.

The Stokes diameters of MPO A and MPO B were determined to be 6.8 ± 0.1 and 5.6 ± 0.1 nm, respectively, by DLS. These results were invariant to protein concentration between 1 and 6 mg/mL. Determinations made in both 8 mM PBS (pH 7.4) and 15 mM Tris (pH 7.5) buffers showed no measurable difference in the Stokes diameter. Thus, the Stokes diameters are consistent with the trend in SEC elution which indicated a larger hydrodynamic size for MPO A.

The sedimentation coefficient (s) and the diffusion coefficient (D) of MPO A and MPO B were obtained by fitting the experimental sedimentation velocity profiles. The sedimentation coefficients measured in 15 mM Tris (pH 7.5) were determined to be 2.457 and 2.695 S for MPO A and MPO B, respectively, while the diffusion coefficients were 6.59×10^{-7} cm^2/s for MPO A and 7.56×10^{-7} cm^2/s for MPO B. The Stokes diameters calculated from the diffusion coefficients are 6.48 nm for MPO A and 5.64 nm for MPO B. Measurement of the Stokes diameter of MPO A prepared in 8 mM PBS yielded a value, 6.84 nm, slightly larger than that determined in 15 mM Tris buffer. However, the difference between the values is not significant and is within the expected experimental uncertainty for the measurements. Application of a prolate ellipsoid model for the protein shape in solution (*29*) resulted in a maximum axial ratio, $(a/b)_{p,m}$, of 8.5 for MPO A and 5.6 for MPO B. The excellent agreement between DLS and SV data definitively establishes the larger hydrodynamic size of MPO A relative to MPO B. Moreover, the sedimentation equilibrium, which provides a means of validating that the interpretation of the hydrodynamic sizes is not complicated by the formation of oligomers, gave no indication of nonideal effects perturbing the measured molecular mass. These findings unambiguously conclude that both proteins were monomeric under the solution conditions used to determine the hydrodynamic size and shape, and therefore, the difference in the hydrodynamic sizes truly reflects the molecular shape difference among the MPO molecules.

NMR Spectroscopy. To further characterize possible structural differences among the chimeras, we compared the one-dimensional proton NMR spectra of two MPO molecules that exhibited the lowest- and highest-affinity modulation in TF-1 binding, i.e., MPO A and MPO B. Despite the high molecular mass, the upfield regions of the NMR spectra are relatively well-resolved and can be characterized using one-dimensional NMR methods (Figure 3). Although the NMR resonances of SynIL-3 A and SynIL-3 B have not been fully assigned, the upfield regions of the spectra are analogous to those of the previously assigned SC-65369 spectrum (*23*), another engineered IL-3 receptor agonist. Therefore, the resonances at <0.0 ppm in the spectra of SynIL-3 A and SynIL-3 B most likely arise from the methyl groups of Leu-68 and Leu-111.

For the upfield region, the spectrum of an equimolar mixture of SynIL-3 B, G-CSF (S17), and linker L2 (Figure 3C or 3I) is remarkably similar to the summed spectra for the individual agonist proteins (panels A and B or G and H of Figure 3). However, when these spectra are compared with that of MPO B at pH 7 (Figure 3E), the latter is significantly different. This spectral difference was present independent of MPO B concentration in the range of 0.07−0.5 mM. Addition of KCl to a final concentration of 100 mM resulted in some precipitation, while there is no change in the spec-

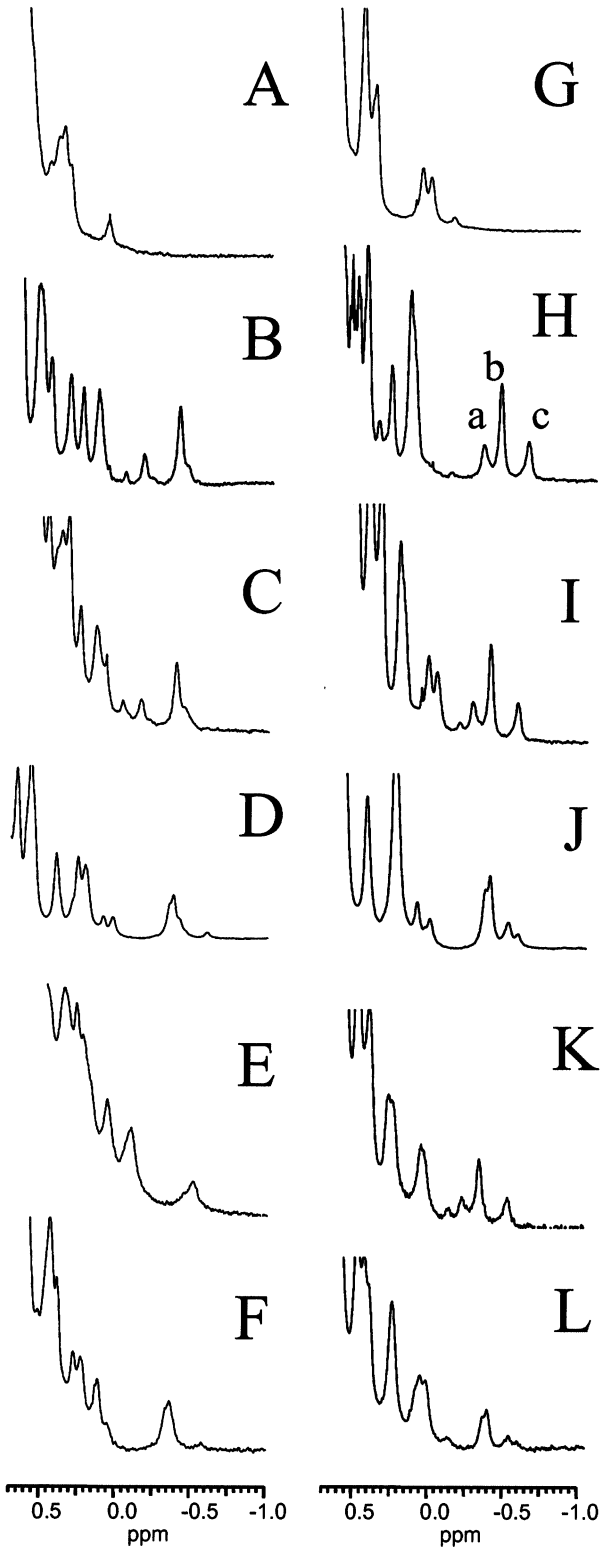

FIGURE 3: One-dimensional ^{1}H NMR spectra of the following samples at pH 7.0 and 4.0, respectively: G-CSF (S17) (A and G), SynIL-3 B (B and H), an equal molar mixture of G-CSF (S17), SynIL-3 B, and L2 (C and I), SynIL-3 A (D and J), MPO B (E and K), and MPO A (F and L). Peaks a and c are likely to arise from the methyl groups of Leu-68 in SynIL-3 B, and peak b is proposed to arise from the methyl groups of Leu-111 in SynIL-3 B.

trum. In contrast, the MPO B spectrum at pH 4 (Figure 3K) is similar to the summed spectra for the individual proteins (Figure 3G,H) or the spectrum of the mixture of SynIL-3 B, G-CSF (S17), and linker L2 (Figure 3I) acquired under the same conditions. When the same experiments were carried out for MPO A (Figure 3F,L), no spectral changes were observed when compared with the corresponding components (Figure 3A,D,G,J).

Despite the spectral change in side chain resonances, the preservation of the backbone structure of the individual domains in MPO B is revealed by its ^{15}N−^{1}H HSQC spectrum, which is sensitive to subtle changes in main chain conformations. The ^{15}N−^{1}H HSQC spectrum of MPO B bears much resemblance to the overlay spectrum of the two component domains (data not shown), although the chimera spectrum exhibited significant line broadening. This is a strong indication that the conformation of the individual components in the chimera is largely preserved as they are in isolated domains. Thus, the spectral changes in side chain resonances of MPO B are likely to reflect a conformational change involving only a localized area of the structure. The ^{15}N−^{1}H HSQC spectrum of MPO A (data not shown) was also similar to the overlay spectrum of the involved components.

DISCUSSION

We have taken advantage of a series of recombinant chimeric myelopoietin molecules to study the structure−activity relationships of these molecules. MPOs are capable of binding to and activating both the IL-3 and G-CSF receptors. Ligand binding and subsequent signaling through the receptors are paramount for these MPOs to carry out their biological functions. All MPOs that have been analyzed bind to both the high-affinity $\alpha\beta$ IL-3 receptor expressed on TF-1 cells and the low-affinity IL-3 receptor α-subunit. The kinetic data show that the dissociation rates of the myelopoietin chimeras from the α-subunit were uniformly, approximately, 2-fold slower than the rates of their cognate IL-3 receptor agonist counterpart. These slower dissociation rates of the myelopoietins may be explained, in part, by their larger radii which would translate to a decreased rate of diffusion. Consequently, further differences in relative binding affinity between a myelopoietin and a corresponding IL-3 receptor agonist to the α-subunit would depend primarily upon the association rate. These relative differences in binding affinity become significantly more pronounced at the heteromultimeric $\alpha\beta$ IL-3 receptor on TF-1 cells. On TF-1 cells, the potency of binding of the MPOs to the IL-3 receptor is not proportional to that of their corresponding cognate IL-3 receptor agonists. For example, MPO A and MPO B differ primarily in the IL-3 receptor agonist domain, yet they exhibit a 3- and 42-fold decrease in affinity relative to SynIL-3 A and SynIL-3 B, respectively. Thus, as described, in comparison to the cognate IL-3 receptor agonists, MPOs have a decreased affinity of binding to the IL-3 receptor in cells expressing the $\alpha\beta$ IL-3 receptor alone (e.g., TF-1 cells). In contrast, MPO binding to the IL-3 receptor is enhanced in cells which express both IL-3 and G-CSF receptors (*8*). This enhanced IL-3 receptor binding on cells expressing both receptors may be a result of increased avidity due to bivalent binding. The differential binding of the IL-3 receptor agonist in cells expressing IL-3R$_{\alpha/\beta}$ alone compared with the cells expressing IL-3R$_{\alpha/\beta}$ and the G-CSF receptor could result in a novel biological response for the chimera molecule compared with a coaddition (*10*).

A plausible explanation for the large affinity difference observed in TF-1 cells and thus for the differential modulations of association kinetics may be reflected as structural perturbations within the chimera lending itself to different levels of accessibility of the pharmacophore to the binding site. In fact, the small difference between the affinity of SynIL-3 A and that of MPO A is in contrast to the large difference in affinities seen between SynIL-3 B and SynIL-3 C and their respective MPO counterparts. The minimal effect on the IL-3 receptor binding pharmacophore of SynIL-3 A in the context of MPO A, as evidenced from the smaller association and dissociation rate change, indicates that the IL-3 receptor binding pharmacophore of MPO A retains a similar level of accessibility to the IL-3 receptor. The larger difference in affinity between the SynIL-3 B−MPO B and SynIL-3 C−MPO C pairs suggests that the IL-3 receptor binding pharmacophores of SynIL-3 B and SynIL-3 C within these MPOs have become considerably less accessible to the IL-3 receptor. Although our results also suggest a small orientation and linker preference, these results clearly demonstrate that the linker and orientation are not the sole determinants of the receptor binding characteristics of these MPOs, and imply that an interdomain interaction may exist. In other words, upon incorporation into the MPO chimeric molecules, the IL-3 receptor agonists no longer function as independent domains. Instead, they become an integral part of the newly formed molecule, and their properties are differentially modified in the MPO. To our knowledge, this is the first study that investigated the interdomain interaction by varying a building block of a single molecule possessing dual receptor agonist activity. This differential effect was not observed in earlier reports of dual receptor agonists in which the focus was only on linker and orientation effects (*15*, *16*). The library of engineered IL-3 receptor agonists offered a unique opportunity to investigate this aspect of the chimeric molecules.

Spectroscopic and conformational studies support the hypothesis that structural features may be responsible for the differential effect on the rate of association of the MPOs to the IL-3 receptor. Structural perturbations upon formation of MPO B, MPO C1, and MPO C2 were implied in their near-UV CD spectra, where a large change in ellipticity occurs at 281 nm. The specific positive resonances at 281 nm are indicative of a more ordered structure in the tyrosine/tryptophan environment. Since the fluorescence emission spectra, which are dominated by the tryptophans, indicate that the tryptophans are in similar microenvironments in both the chimeras and the isolated domains (R. Schilling and C. Jarvis, unpublished data), the nonadditivity of the near-UV CD spectra is suggested to result from changes in the environment surrounding the aromatic residues in the chimeras.

The NMR data provide another line of evidence, in agreement with the near-UV CD results, consistent with structural differences among MPOs containing different IL-3 receptor agonists. Changes between the side chain resonances of MPO B and those of the corresponding components were detected at pH 7, while little change was observed for the same chimera at pH 4 or for MPO A at either pH. The presence of the linker in MPO B apparently does not result in such a spectral change. The lack of the MPO B spectral change at pH 4, nevertheless, suggests that this change is due to electrostatic interaction(s) which is missing in MPO A. These biophysical properties of the MPOs measured by CD and NMR at neutral pH appear to correlate with the changes in the affinity of binding of these MPOs to the IL-3 receptor relative to their cognate IL-3 receptor agonists, which are also measured at neutral pH. On the other hand, the resemblance of the far-UV CD and the two-dimensional $^{1}H-^{15}N$ HSQC spectra of MPO A and MPO B to the sum or overlay spectra of the individual domains suggests a lack of gross structural changes in these domains within the chimeras. This observation, however, does not rule out changes that occur at the tertiary structural level which may limit the accessibility of the IL-3 receptor binding pharmacophores.

The size exclusion chromatographic elution patterns are consistent with differences in molecular shape, with MPO B being more compact than MPO A and the MPO C series being intermediate. The absolute molecular mass/molecular size analyses via DLS, SV, and SE conclusively demonstrate that MPO A has an elongated structure compared to MPO B, with the hydrodynamic diameter of MPO B ∼20% smaller than that of MPO A. The increased compactness of these MPO molecules is consistent with interdomain interactions and potentially explains decreased access of the IL-3 receptor binding pharmacophore to the receptors and correlates with a trend toward lower IL-3 receptor binding affinity. The most compact MPO molecule, i.e., MPO B, exhibited the largest decrease (42-fold) in IL-3 receptor potency relative to its corresponding IL-3 receptor agonist. By comparison, MPO A, the least compact MPO molecule, displayed binding properties similar to those of its cognate IL-3 receptor agonist. While the studies reported herein suggest structural differences in MPO molecules, conclusive identification of the specific changes in MPO conformation awaits X-ray structural determination.

In summary, we have shown that the IL-3 receptor binding affinity of the IL-3 receptor agonists is modulated by the presence of the G-CSF receptor agonist in the chimera, and that interdomain interactions are at least partially responsible for the modulation. This finding revealed another dimension to explore when constructing bifunctional molecules. It demonstrates that the possibility of the functional domains influencing each other in a chimera is a variable to consider in addition to the linker and orientation effect to optimize dual receptor agonists.

ACKNOWLEDGMENT

We gratefully acknowledge Kam Fok and Mark Nagy of the Protein Core Lab for their synthesis of the two linker proteins, L1 and L2, and Iris Leung for technical assistance in obtaining the linker CD spectra.

REFERENCES

1. Schrader, J. W. (1986) *Annu. Rev. Immunol. 4*, 205−230.
2. Metcalf, D. (1991) *Science 254*, 529−533.
3. Nicola, N. A., Metcalf, D., Matsumoto, M., and Johnson, G. R. (1983) *J. Biol. Chem. 258*, 9017−9023.
4. Geissler, K., Peschel, C., Niederwieser, D., Strobl, H., Goldschmitt, J., Ohler, L., Bettelheim, P., Kalhs, P., Huber, C., Lechner, K., Hocker, P., and Kolbe, K. (1996) *Blood 87*, 2732−2739.
5. Lemoli, R. M., Rosti, G., Visani, G., Gherlinzoni, F., Miggiano, M. C., Fortuna, A., Zinzani, P., and Tura, S. (1996) *J. Clin. Oncol. 14*, 3018−3025.

6. Huhn, R. D., Yurkow, E. J., Tushinski, R., Clarke, L., Sturgill, M. G., Hoffman, R., Sheay, W., Cody, R., Philipp, C., Resta, D., and Goerge, M. (1996) *Exp. Hematol. 24*, 839−847.
7. MacVittie, T. J., Farese, A. M., Herodin, F., Grab, L. B., Baum, C. M., and McKearn, J. P. (1996) *Blood 87* (10), 4129−4135.
8. Monahan, J. B., Hood, W. F., Joy, W. D., Caparon, M. H., Paik, K., Goldberg, S. B., Klein, B. K., Staten, N. R., Pegg, L. E., Bauer, S. C., Mina, M. S., Abrams, M. A., Hirsch, J. L., Abegg, A. L., Giri, J. G., Baum, C. M., and McKearn, J. P. (1995) *Blood 86* (Suppl. 1), 154a.
9. McKearn, J. P., Hood, W. F., Monahan, J. B., Joy, W. D., Caparon, M. H., Paik, K., Bauer, S. C., Lee, S. C., Goldberg, S. B., Klein, B. K., Staten, N. R., Pegg, L. E., Abrams, M. A., Hirsch, J. L., Abegg, A. L., Donnelly, A. M., Giri, J. G., Tsai, B. S., Keith, R. H., and Baum, C. M. (1995) *Blood 86* (Suppl. 1), 259a.
10. MacVittie, T. J., Farese, A. M., Davis, T. A., Lind, L. B., and McKearn, J. P. (1999) *Exp. Hematol. 27*, 1557−1568.
11. DiPersio, J. F., Abboud, C. N., Winter, J. N., Bensinger, W., Collins, D. M., Peppard, T., Santos, V. R., and Baum, C. M. (1997) *Blood 90* (Suppl. 1), 97a.
12. Abboud, C. N., DiPersio, J. F., Gordon, L., Frenette, G., Denes, A., Collins, D. M., Peppard, T., Santos, V. R., and Baum, C. M. (1997) *Blood 90* (Suppl. 1), 173a.
13. Haylock, D. N., Rohrsheim, J., Minster, N., Wolfe, S. L., McKearn, J. P., To, L. P., and Simmons, P. J. (1999) *Blood 94* (Suppl. 1), 556a.
14. DiFalco, M. R., and Congote, L. F. (1997) *Biochem. J. 326*, 407.
15. Curtis, B. M., Williams, D. E., Broxmeyer, H. E., Dunn, J., Farrah, T., Jeffery, E., Clevenger, W., DeRoos, P., Martin, U., Friend, D., Craig, V., Gayle, R., Price, V., Cosman, D., March, C. J., and Park, L. S. (1991) *Proc. Natl. Acad. Sci. U.S.A. 88*, 5809−5813.
16. Weich, N. S., Tullai, J., Guido, E., McMahon, M., Jolliffe, L. K., Lopez, A. F., Vadas, M. A., Lowry, P. A., Quesenberry, P. J., and Rosen, J. (1993) *Exp. Hematol. 21*, 647−655.
17. Zhao, C. H., Tang, P. H., Wang, J. X., Mao, N., Kiang, F., Li, X. S., Liu, X. Z., Zhang, M. W., Ren, Y. F., and Du, D. L. (1994) *Stem Cells (Miamisburg, Ohio) 12*, 339−347.
18. Rock, F., Everett, M., and Klein, M. (1992) *Protein Eng. 5* (6), 583−591.
19. Klemsz, M., Kaushansky, K., Cooper, R., Cooper, S., Broxmeyer, H., and Hromas, R. (1996) *Blood 88* (Suppl. 1), 544a.
20. Olins, P. O., Bauer, S. C., Bradford-Goldberg, S., Sterbenz, K., Polazzi, J. O., Caparon, M. H., Klein, B. K., Easton, A. M., Paik, K., Klover, J. A., Thiele, B. R., and McKearn, J. P. (1995) *J. Biol. Chem. 270*, 23754−23760.
21. Thomas, J. W., Baum, C. M., Hood, W. F., Klein, B. K., Monahan, J. B., Paik, K., Staten, N., Abrams, M., and McKearn, J. P. (1995) *Proc. Natl. Acad. Sci. U.S.A. 92*, 3779−3783.
22. McWherter, C. A., Feng, Y., Zurfluh, L. L., Klein, B. K., Baganoff, M. P., Polazzi, J. O., Hood, W. F., Paik, K., Abegg, A. L., Grabbe, E. S., Shieh, J., Donnelly, A. M., and McKearn, J. P. (1999) *Biochemistry 38*, 4564−4571.
23. Feng, Y., Klein, B. K., Vu, L., Aykent, S., and McWherter, C. A. (1995) *Biochemistry 34*, 6540−6551.
24. Laemmli, U. K. (1970) *Nature 227*, 680−685.
25. Fasman, G. D., Ed. (1976) in *Handbook of Biochemistry and Molecular Biology*, 3rd ed., Vol. 1, Proteins, pp 185−199, CRC Press, Boca Raton, FL.
26. Philo, J. (1994) in *Modern Analytical Ultracentrifugation* (Schuster, T. M., and Laue, T. M., Eds.) pp 156−170, Birkhauser, Boston.
27. Philo, J. (1997) *Biophys. J. 72*, 435−444.
28. Johnson, M. L., Correia, J. J., Yphantis, D. A., and Halvorson, H. R. (1981) *Biophys. J. 36*, 575−588.
29. Laue, T. M., Shah, B. D., Ridgeway, T. M., and Pelletier, S. (1992) in *Analytical Ultracentrifugation in Biochemistry and Polymer Science*, pp 90−125, Redwood Press Ltd., Melksham.
30. Liu, M., Mao, X., Ye, C., Huang, H., Nicholson, J. K., and Linaon, J. C. (1998) *J. Magn. Reson. 132*, 125−129.
31. Zhang, O., Kay, L. E., Olivier, J. P., and Forman-Kay, J. D. (1994) *J. Biomol. NMR 4*, 845−858.
32. Monahan, J. B., Hood, W. F., Welply, J. K., Shieh, J. J., Polazzi, J. O., and Li, X. (2001) *Exp. Hematol.* (in press).
33. Klein, B. K., Feng, Y., McWherter, C. A., Hood, W. F., Paik, K., and McKearn, J. P. (1997) *J. Biol. Chem. 272*, 22630−22641.
34. Klein, B. K., Olins, P. O., Bauer, C., Caparon, M. H., Easton, A. M., Braford-Goldberg, S., Abrams, M. A., Klover, J. A., Paik, K., Thomas, J. W., Hood, W. F., Shieh, J. J., Polazzi, J. O., Donnelly, A., Zeng, D. L., Welply, J. K., and McKearn, J. P. (1999) *Exp. Hematol. 27*, 1746−1756.
35. Kitamura, T., Sato, N., Arai, K., and Miyajima, A. (1991) *Cell 66*, 1165−1174.
36. Metcalf, D., and Nicola, N. A. (1995) *The Hemopoietic Colony-stimulating Factors: from Biology to Clinical Applications*, Cambridge University Press, Cambridge, U.K.
37. Strickland, E. H. (1974) *Crit. Rev. Biochem. 2*, 113−175.

BI010590T